Ultraviolet Photolysis of the ClO Dimer

J. Plenge,[†] R. Flesch,[‡] and S. Kühl[§]

Fachbereich Physik, Universität Osnabrück, Barbarastrasse 7, 49069 Osnabrück, Germany

B. Vogel, R. Müller, and F. Stroh

Forschungszentrum Jülich, Institut für Stratosphärische Chemie (ICG I), 52425 Jülich, Germany

E. Rühl*

Institut für Physikalische Chemie, Universität Würzburg, Am Hubland, 97074 Würzburg, Germany

Received: January 21, 2004; In Final Form: April 1, 2004

Photodissociation of the ClO dimer (ClOOCl) is studied in the ultraviolet regime (250 and 308 nm) under collision-free conditions. The primary photolysis products are probed by photoionization mass spectrometry. At both photolysis wavelengths, exclusively the formation of $2Cl + O_2$ is observed, corresponding to a primary quantum yield γ_{Cl} near unity. Considering the error limit of the experimental results one obtains $\gamma_{Cl} \geq 0.98$ at 250 nm and $\gamma_{Cl} \geq 0.90$ at 308 nm, respectively. At both photolysis wavelengths the pathway yielding ClO is *not* observed, corresponding to $\gamma_{ClO} \leq 0.02$ at 250 nm and $\gamma_{ClO} \leq 0.10$ at 308 nm. Sensitivity studies of these results with respect to ozone depletion in the stratosphere regarding photochemically induced ozone loss are discussed using model simulations. These simulations suggest that a change of γ_{Cl} from 1.0 to 0.9 leads to a reduction of polar ozone loss of ∼5%.

Introduction

Numerous theoretical and experimental studies have been devoted to the stability, spectroscopy, and photochemistry of the ClO dimer (Cl_2O_2). These are mainly motivated by the observation of strong stratospheric ozone loss in polar spring.[1] A catalytic reaction cycle involving Cl_2O_2 is believed to play an important role:[2]

$$2ClO + M \rightleftharpoons Cl_2O_2 + M \quad (1)$$

$$Cl_2O_2 + h\nu \rightarrow ClOO + Cl \quad (2)$$

$$ClOO + M \rightarrow Cl + O_2 + M \quad (3)$$

$$2(Cl + O_3 \rightarrow ClO + O_2) \quad (4)$$

$$2O_3 + h\nu \rightarrow 3O_2 \quad (5)$$

In addition to the photolysis channel (2), Cl_2O_2 may undergo a competitive photolysis pathway leading to ClO formation:

$$Cl_2O_2 + h\nu \rightarrow 2ClO \quad (6)$$

This reaction leads to a null cycle in the balance of atmospheric ozone. Its atmospheric relevance was discussed by Eberstein and Minton et al.[3,4]

Several theoretical studies have been carried out to investigate the structure, stability, and photochemistry of the ClO dimer.[5−10] According to these works, Cl_2O_2 occurs most likely in the stratosphere as dichlorine peroxide (ClOOCl), whereas other isomers, such as ClOClO or $ClClO_2$, are believed to be less stable. The photolysis of ClOOCl yielding $2Cl+O_2$ is the dominant process, whereas only small amounts of ClO are formed at short ultraviolet (UV)-photolysis wavelengths.[9] The quantum yield for 2ClO formation is calculated to be zero below 4.4 eV photon energy. It reaches 0.05 in the 4.4−5.0 eV regime (248 nm $\leq \lambda \leq$ 282 nm). Kaledin and Morokuma studied the photodissociation dynamics of ClOOCl considering the synchronous and sequential formation of $2Cl+O_2$ at 308 nm, and there are three fragmentation routes at 248 nm yielding $2Cl + O_2$, $Cl + O + ClO$, and $2Cl + 2O$, respectively.[10]

First experiments on the photolysis of ClOOCl indicated that primarily atomic chlorine is formed at 254 nm.[11] This result was confirmed for 308 nm, where a quantum yield close to unity ($\gamma_{Cl} = 1.03 \pm 0.12$) was reported for Cl formation.[12] More recently, Moore et al. found experimental evidence for the photolysis channel according to eq 6.[13] They deduced from molecular beam experiments a 9:1 preference for the formation of $2Cl + O_2$ (cf. channel (2)), where photolysis experiments were carried out at 248 and 308 nm, respectively. Specifically, they reported for the photolysis at 248 nm: $\gamma_{Cl} = 0.88 \pm 0.07$ and $\gamma_{ClO} = 0.12 \pm 0.07$. For the photolysis at 308 nm the following values are reported: $\gamma_{Cl} = 0.9 \pm 0.1$ and $\gamma_{ClO} = 0.1 \pm 0.1$,[13] where the quantum yields of both channels (2) and (6) add to unity.

The present study aims to use a novel pump−probe laboratory approach for the reliable detection of the primary photofragments of the ClO dimer including their branching ratio at various ultraviolet wavelengths. Model simulations are performed to

* Corresponding author. Phone: ++49-931-888 6300. Fax: ++49−931−888 6302. E-mail: eruehl@phys-chemie.uni-wuerzburg.de.

[†] Present address: Department of Chemistry, University of California at Berkeley

[‡] Present address: Institut für Physikalische Chemie, Universität Würzburg, Germpany

[§] Present address: Institut für Umweltphysik, Universität Heidelberg, Germany

10.1021/jp049690+ CCC: $27.50
Published on Web 05/12/2004

emphasize the atmospheric implications of the results from laboratory work.

Experimental Section

The experimental setup consists of the following components: (i) a flow tube for the efficient ClO and ClO dimer production (cf. ref 14); (ii) an excimer-pumped dye laser (Lambda Physik: LPX 202 and Scanmate) equipped with a frequency doubling unit (BBO(I)-crystal); and (iii) a time-correlated, tunable vacuum-ultraviolet (VUV) radiation source (laser-produced plasma), which is typically delayed by 100 ns with respect to the primary photolysis pulse. It delivers radiation pulses of 25 ns length (typically 10^9 photons/s) in the energy regime 8 eV$\leq E \leq$ 25 eV (155 nm $\geq \lambda \geq$ 50 nm, photon bandwidth $\Delta\lambda = 0.8$ nm) and (iv) a time-of-flight mass spectrometer (TOF) for cation separation and detection. Further details have been published elsewhere.[15]

ClO is generated in the flow tube by the following reaction: $Cl + OClO \rightarrow 2ClO$. We used a gas mixture of 5% Cl_2 in He for Cl production in a microwave discharge at typically $p = 5$ hPa. The OClO source has been described before.[16] The formation of Cl_2O_3 is avoided by keeping the OClO partial pressure as low as possible, so that $Cl_2O_3^+$ (*m*/*z* 118, 120, 122) is not observed in photoionization mass spectra. This implies using an excess of atomic chlorine relative to OClO. The ClO dimer is efficiently produced by cooling the flow tube to 170 K. It is known that the rate constant of the above-mentioned reaction Cl + OClO is only slightly temperature dependent, which increases most likely with decreasing temperature.[17] We assume that the ClO dimer in the sample is mostly ClOOCl. This assignment is in agreement with earlier work.[18] There are also contributions from $ClClO_2$. Evidence for this species is found from the mass signals of ClO_2^+ (*m*/*z* 67, 69). Photoion yields of ClO_2^+ have been recorded by selecting these mass signals, while scanning the VUV energy. As a result, the appearance energy (AE) of these cations is found at 11.34 $\pm$ 0.05 eV, which is well above the ionization energy (IE) of OClO (IE = 10.35 eV).[16] The AE is in excellent agreement with the ionic fragmentation process $ClClO_2^+ \rightarrow ClO_2^+ + Cl + e^-$, using data from ref 19. We estimate from the photolysis experiments, which are described in the following, that the Cl_2O_2 sample contains 83 $\pm$ 2% ClOOCl and 17 $\pm$ 2% $ClClO_2$. Evidence for the formation of higher chlorine oxides is not found.

The gaseous sample emerges from the flow tube into a high vacuum recipient, where the ionization region of the TOF is located. There, the photolysis and the photoionization light pulses are spatially overlapped. The pressure in the ionization region is $\sim 10^{-3}$ Pa, so that the photolysis occurs under collision-free conditions and primary photofragments are detected. The photon flux of the photolysis pulse is kept low (<30 mJ/cm^2) to avoid multiphoton excitation and ionization.

The photolysis experiments are carried out at 250 and 308 nm, respectively. These wavelengths were chosen in order to compare the present results to earlier experimental works.[11−13] A typical set of photoionization mass spectra at a given UV-photolysis wavelength and VUV-photon energy consist of (i) photoionization by VUV-radiation without primary photolysis, (ii) UV-photoexcitation without subsequent VUV-photoionization, so that possible contributions from multiphoton ionization are identified, and (iii) primary UV-photolysis followed by subsequent VUV-photoionization. Data reduction is carried out by subtracting the mass spectra (i) and (ii) from the pump−probe TOF mass spectrum (iii). The resulting difference mass spectra are termed *photolysis mass spectra* in the following, since all mass signals are exclusively due to the primary UV-photolysis processes. Positive mass signals correspond to species that are formed by photolysis, and negative cation intensity is observed for those species that are consumed by photolysis, if contributions from ionic fragmentation are absent.

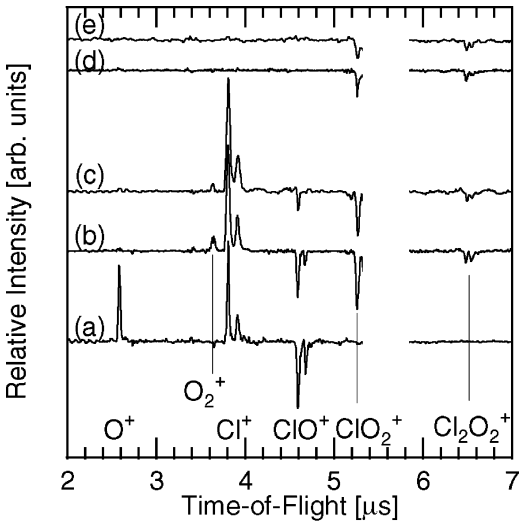

Figure 1. Photolysis mass spectra of ClO and the ClO dimer. The photolysis wavelengths λ are given in nm, the VUV photon energies *E* that are used for photoionization are given in eV. Experimental conditions: (a) $T = 298$ K, $\lambda = 250$ nm, $E = 13.45$ eV; (b) $T = 170$ K, $\lambda = 250$ nm, $E = 13.45$ eV; (c) $T = 170$ K, $\lambda = 308$ nm, $E = 13.45$ eV; (d) $T = 170$, $\lambda = 250$ nm, $E = 11.43$ eV; (e) $T = 170$ K, $\lambda = 308$ nm, $E = 11.43$ eV.

About 20% of the parent species, ClO and Cl_2O_2, are typically photolyzed at 250 nm, as inferred from the change of the parent cation mass signals. The photolysis yield is smaller at longer photolysis wavelengths, i.e., at 308 nm, as a result of the decreased photoabsorption cross section of both species (cf. refs 19 and 20).

Results and Discussion

Ultraviolet Photolysis of the ClO Dimer. Photolysis experiments of the ClO dimer are carried out at 250 and 308 nm. Figure 1 shows a series of photolysis mass spectra: Figure 1a shows the photolysis of ClO ($T = 298$ K) at 250 nm, yielding $Cl(^2P_{3/2}) + O(^1D)$.[21,22] Intense positive mass signals are due to photoionization of these atomic photolysis products. The VUV photon energy is set to 13.45 eV because $O(^1D)$ is probed selectively at this photon energy by autoionization.[23] The *negative* intensity of ClO^+ indicates that ClO is consumed by UV-photolysis. The following changes are observed after cooling the flow system to 170 K, where no free ClO is detected (see Figure 1b): (i) the intense O^+ signal has vanished; (ii) an additional mass signal, corresponding to O_2^+, occurs; (iii) mass signals with negative intensity are detected for ClO_2^+ and $Cl_2O_2^+$; and (iv) a substantial Cl^+ signal is found.

The lack of an O^+ signal indicates that there is little free ClO in the sample. The occurrence of Cl^+ together with O_2^+ gives evidence for reaction 2. It is possible that an intermediate ClOO is formed by UV-photolysis of ClOOCl, which is subsequently photoionized, yielding $Cl + O_2^+$. However, it is known that the ClOO is photolytically formed in an excited state that readily decomposes into $Cl + O_2$ in the femtosecond time regime.[9] As a result, any ClOO that is formed as an intermediate via photolysis will be probed as channel (2). This also implies that the present setup is not well-suited to distinguish between the simultaneous and sequential decay dynamics of ClOOCl.

Cl_2O_2 is consumed by UV-photolysis, yielding a negative $Cl_2O_2^+$ signal in the photolysis mass spectrum (cf. Figure 1b). The negative ClO_2^+ signal shows that $ClClO_2$ is present in the cold flow system (cf. ref 14). The intense Cl^+ signal under cold conditions, where nearly all ClO radicals are bound in ClOOCl, indicates that the ClOOCl is efficiently photolyzed into 2Cl + O_2 (cf. eq 2). The relevance of the competing photolysis channel (6) cannot be reliably deduced from Figure 1b, since the ClO^+ intensity is negative. This finding is rationalized as follows: (i) ClOOCl is photolyzed, so that there is less of this species in the gas phase yielding a weaker ClO^+ signal from fragmentation of $ClOOCl^+$ and (ii) if ClOOCl photolyzes into 2ClO via eq 6, then the nascent ClO must contribute to a *positive* ClO^+ signal. The experimental ClO^+ intensity is expected to be the sum of both contributions. However, it is not possible to evaluate from Figure 1b the amount of nascent ClO that is photoionized. Therefore, Figure 1b is only sensitive to photolysis channel (2). This is similar to Figure 1c, where the photolysis wavelength is set to 308 nm, indicating that there are minor visible changes in photolysis behavior as a function of UV wavelength. However, a specific indicator for the occurrence of different Cl_2O_2 isomers, such as ClOOCl and $ClClO_2$, is the ratio of the mass lines of Cl^+ (*m*/*z* 35, 37) and O_2^+ (*m*/*z* 32): $I_{Cl^+}/I_{O_2^+}$. These cations are formed via photolysis of ClOOCl, yielding after photoionization of the corresponding neutrals $2Cl^+ + O_2^+$, whereas the photolysis of $ClClO_2$ contributes to the Cl^+ and $OClO^+$ signals. Note that changes to the $OClO^+$ signal by photoionization of nascent OClO that is formed from photolyzed $ClClO_2$ cannot be analyzed. This is due to the formation of $OClO^+$ via fragmentation of $ClClO_2^+$ without primary photolysis. As a result of both contributions a negative $OClO^+$ -mass signal is found in the photolysis mass spectra (see Figure 1, parts b and c). We observe at 250 nm and subsequent photoionization at 13.45 eV that $I_{Cl^+}/I_{O_2^+} = 9.6 \pm 1.4$. At 308 nm we obtain from Figure 1c $I_{Cl^+}/I_{O_2^+} = 36 \pm 4$. Note that a pure sample of ClOOCl would give at both photolysis wavelengths the same ratio $I_{Cl^+}/I_{O_2^+} = 8$, using the stoichiometry of channel (2) along with the known photoionization cross sections $\sigma(O_2) = 6$ Mb,[24] $\sigma(Cl) = 24$ Mb[25] at 13.45 eV. This cation ratio implies that both photolysis products are formed in their ground state. The experimental results indicate that there are evidently different species present that change $I_{Cl^+}/I_{O_2^+}$. Using the photoionization cross section of the neutral photolysis products at 13.45 eV, considering the bandwidth of the LPP radiation source, as well as the absorption cross sections at both photolysis wavelengths,[20,26] we obtain that $83 \pm 2\%$ of the Cl_2O_2 species in the sample are due to ClOOCl, whereas $17 \pm 2\%$ correspond to $ClClO_2$, as already mentioned above. The presence of $ClClO_2$ contributes about 12% to the Cl^+ mass signal via UV-photolysis at 250 nm and subsequent photoionization at 13.45 eV. Note that this situation changes at 308 nm, where the contribution of $ClClO_2$ to the Cl^+ signal is dominant, so that only ~30% of this mass signal comes from the photolysis of ClOOCl.

The relevance of channel (6) is determined by reducing the VUV photon energy to 11.43 eV (cf. Figure 1, parts d and e). This photon energy is below the threshold of ionic fragmentation of ClOOCl. The appearance energy of ClO^+ from ClOOCl is calculated to be 11.60 ± 0.08 eV. The photoionization cross section of ClO is known to be 15 ± 2 Mb at 11.5 eV,[25] so that any ClO is sensitively detected by photoionization mass spectrometry, if it is formed via eq 6. The sensitivity of ClO detection is expected to be further increased by about 10%, if ClO is formed vibrationally excited upon photolysis. This is a result of an increased photoionization cross section of vibrationally excited ClO (cf. ref 27). Figure 1d clearly shows that there is *no* evidence for ClO^+, if the photolysis wavelength is set to 250 nm. Identical results are obtained from photolysis experiments at 308 nm (see Figure 1e), but the signal-to-noise ratio is lower as a result of the small absorption cross section of ClOOCl at 308 nm ($\sigma_{308nm} = 0.341$ Mb; $\sigma_{250nm} = 5.889$ Mb[20]). The present results indicate that there is *no* evidence for photolysis channel (6). This implies that we can only determine an upper limit of the primary quantum yield for 2ClO formation γ_{ClO}. This quantity is mostly limited by the signal-to-noise ratio and the signal strengths of the experimental data, as will be outlined below. We assume that each UV photon absorbed by ClOOCl leads to photodissociation, according to the possible channels (2) and (6). As a result, the quantum yields of both channels add to unity. This assumption appears to be justified, since there are no other processes known to occur upon UV-excitation of ClOOCl (cf. ref 13) and electronically excited ClOOCl is unlikely to undergo a radiative decay via the emission of fluorescence photons. The primary quantum yield for 2Cl formation γ_{Cl} and 2ClO formation γ_{ClO} depends on the mass spectrometric intensities *I* and the photoionization cross sections σ as follows:

$$\gamma_{Cl} = (I_{Cl^+}/\sigma_{Cl})/[(I_{Cl^+}/\sigma_{Cl}) + (I_{ClO^+}/\sigma_{ClO})] \quad (7)$$

and

$$\gamma_{ClO} = (I_{ClO^+}/\sigma_{ClO})/[(I_{Cl^+}/\sigma_{Cl}) + (I_{ClO^+}/\sigma_{ClO})] \quad (8)$$

An estimate for the error limits of both quantum yields γ_{Cl} and γ_{ClO} is essential to quantify the quality of the present results in comparison with previous works.[12,13] This is accomplished by considering the detection limits of both cations. The estimate of the detection limits is based on the cation signals strengths that are measured as voltage pulses by a digital oscilloscope, where the signals are loaded into 50 Ω. We observe no ClO^+ intensity in the experimental time-of-flight mass spectra (Figure 1d,e), where the standard deviation σ of the cation background signal corresponds to 0.05 ± 0.01 (see Figure 1d) and 0.135 ± 0.045 mV (see Figure 1e), respectively. Furthermore, we use as a detection limit 3σ, which is 0.15 mV at 250 nm and 0.405 mV at 308 nm, respectively. The ratio between the detected cation intensity and the corresponding photoionization cross section is proportional to the number of neutral photolysis products in the ionization region. This corresponds to 0.027 mV per Mb photoionization cross section of ClO for the primary photolysis at 308 nm (cf. Figure 1e). Similarly, one obtains for the detection of atomic chlorine at the same photolysis wavelength via photoionization mass spectrometry 0.228 mV per Mb photoionization cross section of atomic chlorine (see Figure 1c). As a result of this estimate, we obtain for the photolysis of ClOOCl at 308 nm using eq 8 as an upper limit $\gamma_{ClO} \leq 0.10$. This corresponds to $\gamma_{Cl} \geq 0.90$, assuming that both quantum yields add to unity. The same estimate yields for the primary photolysis at 250 nm: $\gamma_{ClO} \leq 0.02$, so that $\gamma_{Cl} \geq 0.98$. Note that the results are not affected by the photon energy that is used for photoionization, since only I/σ ratios appear in eqs 7 and 8, which are independent of the photon energy after appropriate normalization to the photon flux and the monochromator bandwidth. Possible systematic errors from the presence of species, which lead to Cl formation upon UV-photolysis, are considered as follows: Weak contributions to I_{Cl^+} from Cl_2, which remain from Cl production, have been subtracted prior to the data analysis. These are negligible at

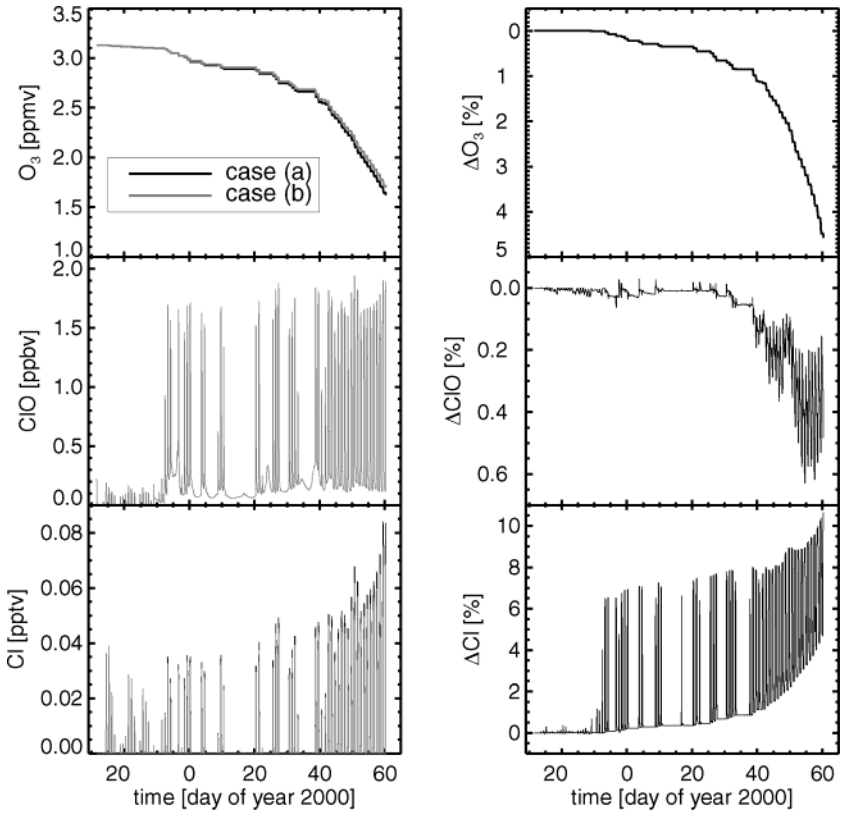

Figure 2. Model simulations for the time period between December 3, 1999 and March 1, 2000 using the CLaMS model at a potential temperature of 475 K. Cases a ($\gamma_{Cl} = 1$) and case b ($\gamma_{Cl} = 0.9$, $\gamma_{ClO} = 0.1$) consider the mixing ratios of ozone (top), ClO (middle), and Cl (bottom). The left-hand patterns show the calculations for cases a and b. The right-hand patterns show the relative change between both cases.

250 nm, since the absorption cross section of Cl_2 is known to be $\sim 4 \times 10^{-4}$ Mb at 250 nm.[28] As a result, this source of atomic chlorine is much less efficient than ClOOCl ($\sigma_{ClOOCl} = 5.889$ Mb at 250 nm[20]). Other sources contributing to I_{Cl^+}, such as OClO, are also expected to be quite weak at 250 nm ($\sigma_{OClO} \approx 0.2$ Mb). However, this situation changes at 308 nm, where the absorption cross sections of impurities, such as $ClClO_2$, increase relative to that of ClOOCl, as outlined above. This leads, together with the low absorption cross section of ClOOCl, to a significantly increased error limit of γ_{ClO}.

The present results indicate that the error limits of the primary quantum yields of the ClO-dimer photolysis channels are considerably smaller at 250 nm than in previous work.[13] At 308 nm we derive a somewhat larger error limit than at 250 nm, which is similar to previous works.[12,13] This is essentially due to impurities in the ClO-dimer sample, which are difficult to avoid. They contribute efficiently to photoionization of the photolysis products of Cl_2O_2. The present work yields no evidence for ClO formation via eq 6. This is unlike previous work, where ClO is clearly identified as a photolysis product at 308 nm.[13] Possible reasons for this discrepancy may be found in the different preparation routes of the ClOOCl compared to ref 13.

Sensitivity Study of the ClO-Dimer Photolysis in the Stratosphere. Photodissociation of the ClO dimer is a key step in one of the dominant catalytic ozone loss cycles, which are responsible for stratospheric ozone depletion in polar spring.[29] Therefore, the results of the present laboratory experiments have direct implications for the understanding of polar ozone loss. These implications are investigated by model simulations with use of γ_{Cl} and γ_{ClO} from the present experiments. We use a box model version of the Chemical Lagrangian Model of the Stratosphere (CLaMS)[30,31] that simulates both the chemistry of multiple air parcels and their transport. This model study is based on simulations[32] of the temporal evolution of chlorine activation and of ozone loss in the Arctic winter 1999/2000. In situ observations of the ClO mixing ratios were obtained from a balloon-borne instrument launched in Kiruna, North Sweden, on March 1, 2000, where quasi-simultaneously measured ozone mixing ratios are available, as well. The measured ClO and ozone mixing ratios are compared to CLaMS simulations, which are initialized for early winter conditions. This allows us to infer the chlorine activation and ozone loss during the winter for altitudes between approximately 13 and 15 km. The model simulations are performed for the time period December 3, 1999 until March 1, 2000 along trajectories taking the diabatic descent into account. At 475 K potential temperature, corresponding to $\sim$20.5 km altitude, full chlorine activation and substantial ozone loss are simulated, which is in agreement with the measurements in the stratosphere. Therefore, we repeat this model simulation at 475 K for case a (ClOOCl exclusively decays via eq 2, i.e., $\gamma_{Cl} = 1.0$) and case b (using $\gamma_{Cl} = 0.9$ and $\gamma_{ClO} = 0.1$). These scenarios are motivated by the error limit given in previous work (cf. ref 13) and the regime of error limits obtained from this work at 308 nm.

Increasing γ_{ClO} should lead to a lower efficiency of the ClO dimer cycle (cf. ref 29). Indeed, we find up to $\sim$5% lower ozone mixing ratios until March 1, 2000 employing case a compared to case b (cf. Figure 2). Furthermore, for given O_3 and CH_4 concentrations, the ratio between Cl and ClO is determined by the ClO dimer photolysis, especially since the NO and O mixing ratios are low in the late winter lower stratosphere. In case a higher Cl mixing ratios are produced, which enhance the ozone destruction rate compared to case b. The model simulations also show that the reaction rate of $Cl + CH_4 \rightarrow CH_3 + HCl$ is higher in case a than in case b. Therefore, more HCl and less CH_4 are

found in case a. Finally, more OH and HO_2 is observed in case a owing to the coupling between chlorine and hydrogen compounds.

In summary, comparing cases a and b one obtains from the simulations a 5−11% greater Cl mixing ratio. This leads to a larger HCl mixing ratio (up to ∼6%) and an insignificant decrease of the CH_4 mixing ratio at the end of the simulation period, whereas differences in the ClO mixing ratios are <1%. Furthermore, approximately 5% more ozone is destroyed when using case a during the Arctic polar winter.

Conclusion

The present results show that the photolysis of the ClO dimer does not lead to any detectable ClO formation. We estimate from the laboratory experiments, considering the signal-to-noise ratios at 250 nm, that $\gamma_{Cl} \geq 0.98$. The competing channel (6) is estimated to be of minor importance, $\gamma_{ClO} \leq 0.02$, if it exists at all. At 308 nm no evicence for photolytic ClO formation is found, as well. The upper limit of $\gamma_{ClO} \leq 0.10$ is a result of the smaller absorption cross section of ClOOCl, which affects the decreased signal-to-noise ratio in photolysis mass spectra. This corresponds to $\gamma_{Cl} \geq 0.90$ at 308 nm. At both photolysis wavelengths ozone depletion proceeds efficiently via reactions 1−4. This result confirms earlier work, where the quantum yield for Cl formation is reported to be unity.[12]

The present results corroborate the conclusions deduced from previous works and reduce the error limit of the primary quantum yield of ClOOCl photolysis. Model simulations yield significant differences for the ozone mixing ratio considering (a) ClOOCl decays exclusively via eq 2, i.e., $\gamma_{Cl} = 1.0$, and (b) $\gamma_{Cl} = 0.9$ and $\gamma_{ClO} = 0.1$. Approximately 5% more ozone is destroyed in case a during the Arctic polar winter than in case b. This is a result of the higher efficiency of the ClO dimer cycle in case a. The efficiency of this cycle is highest under cold sunlit conditions, because at sufficiently high temperature, thermal decomposition of ClOOCl (cf. eq 1) competes with UV-photolysis. Therefore, in particular for Antarctic conditions it is crucial that only the photolysis channel (2) exists.

Acknowledgment. J. Plenge acknowledges financial support by the Deutsche Bundesstiftung Umwelt. Financial support by the Bundesministerium für Bildung und Forschung (BMBF), the European Union, and the Fonds der Chemischen Industrie is gratefully acknowledged.

References and Notes

(1) Farman, J. C.; Gardiner, B. G.; Shanklin, J. D. *Nature* **1985**, *315*, 207.

(2) Molina, L. T.; Molina, M. J. *J. Phys. Chem.* **1987**, *91*, 433.

(3) Eberstein, I. J. *Geophys. Res. Lett.* **1990**, *17*, 721.

(4) Minton, T. K.; Nelson, Ch. M.; Moore, T. A.; Okumura, M. *Science* **1992**, *258*, 1342.

(5) McGrath, P. M.; Clemitshaw, K. C.; Rowland, F. S.; Hehre, W. J. *J. Phys. Chem.* **1990**, *94*, 6126.

(6) Lee, T. J.; McMichael Rohlfing, C.; Rice, J. E. *J. Chem. Phys.* **1992**, *97*, 6593.

(7) Stanton, J. F.; Rittby, C. M. L.; Bartlett, R. J.; Toohey, D. W. *J. Phys. Chem.* **1991**, *95*, 2107. Stanton, J. F.; Bartlett, R. J. *J. Chem. Phys.* **1993**, *98*, 9335.

(8) Zhu, R. S.; Lin, M. C. *J. Chem. Phys.* **2003**, *118*, 4094.

(9) Toniolo, A.; Granucci, G.; Inglese, S.; Persico, M. *Phys. Chem. Chem. Phys.* **2001**, *3*, 4266.

(10) Kaledin, A. L.; Morokuma, K. *J. Chem. Phys.* **2000**, *113*, 5750.

(11) Cox, R. A.; Hayman, G. D. *Nature* **1988**, *332*, 796.

(12) Molina, M. J.; Colussi, A. J.; Molina, L. T.; Schindler, R. N.; Tso, T.-L. *Chem. Phys. Lett.* **1990**, *173*, 310.

(13) Moore, T. A.; Okumura, M.; Seale, J. W.; Minton, T. K. *J. Phys. Chem.* **1999**, *103*, 1691.

(14) Schwell, M.; Jochims, H.-W.; Wassermann, B.; Rockland, U.; Flesch, R.; Rühl, E. *J. Phys. Chem.* **1996**, *100*, 10070.

(15) Flesch, R.; Schürmann, M. C.; Hunnekuhl, M.; Meiss, H.; Plenge, J.; Rühl, E. *Rev. Sci. Instrum.* **2000**, *71*, 1319.

(16) Flesch, R.; Rühl, E.; Hottmann, K.; Baumgärtel, H. *J. Phys. Chem.* **1993**, *97*, 837.

(17) Bemand, P. P.; Clyne, M. A. A.; Watson, R. T. *J. Chem. Soc., Faraday Trans. 1* **1973**, *69*, 1356.

(18) Burkholder, J. B.; Orlando, J. J.; Howard, C. J. *J. Phys. Chem.* **1990**, *94*, 687.

(19) Wayne, R. P.; Poulet, G.; Biggs, P.; Burrows, J. P.; Cox, R. A.; Crutzen, P. J.; Hayman, G. D.; Jenkin, M. E.; Le Bras, G.; Moortgart, G. K.; Platt, U.; Schindler, R. N. *Atmos. Environ.* **1995**, *29*, 2675.

(20) Huder, K. J.; deMore, W. B. *J. Phys. Chem.* **1995**, *99*, 3905.

(21) Flesch, R.; Plenge, J.; Schürmann, M.-C.; Kühl, S.; Klusmann, M.; Rühl, E. *Surf. Rev. Lett.* **2002**, *9*, 105.

(22) Flesch, R.; Plenge, J.; Kühl, S.; Klusmann, M.; Rühl, E. *J. Chem. Phys.* **2002**, *117*, 9663.

(23) Flesch, R.; Schürmann, M. C.; Hunnekuhl, M.; Meiss, H.; Plenge, J.; Rühl, E. *Phys. Rev. A* **2000**, *62*, 52723.

(24) Berkowitz, J. *Photoabsorption, Photoionization, and Photoelectron Spectroscopy*; Academic Press: New York, 1978.

(25) Plenge, J. Ph.D. Thesis, Universität Osnabrück, 2002.

(26) Müller, H.S. P.; Willner, H. *Ber. Bunsen-Ges. Phys. Chem.* **1992**, *96*, 427.

(27) Flesch, R.; Schürmann, M. C.; Plenge, J.; Hunnekuhl, M.; Meiss, H.; Bischof, M.; Rühl, E. *Phys. Chem. Chem. Phys.* **1999**, *1*, 5423.

(28) Maric, D.; Burrows, J. P.; Meller, R.; Moortgat, G. K. *J. Photochem. Photobiol. A* **1993**, *70*, 205.

(29) Anderson, J. G.; Toohey, D. W.; Brune, W. H. *Science* **1991**, *251*, 39.

(30) McKenna, D. S.; Konopka, P.; Grooss, J.-U.; Günther, G.; Müller, R.; Spang, R.; Offermann, D.; Orsolini, Y. *J. Geophys. Res.* **2002**, *107*, 4309.

(31) McKenna, D. S.; Grooss, J.-U.; Günther, G.; Konopka, P.; Müller, R.; Carver, G. *J. Geophys. Res.* **2002**, *107*, 4256.

(32) Vogel, B.; Stroh, F.; Grooss, J.-U.; Müller, R.; Deshler, T.; Karhu, J.; McKenna, D. S.; Müller, M.; Toohey, D.; Toon, G. C. *J. Geophys. Res.* **2003**, *108*, 8334.